3.12. ACKNOWLEDGEMENTS

The laboratory studies of tailings were conducted at CANMET, Ottawa, where technical assistance was generously provided by D.R. Owens (microbeam), P. Carrière (X-ray diffraction), and J.M. Greer (lapidary). Much of the work was done in collaboration with D.W. Blowes of the Waterloo Centre for Groundwater Research, University of Waterloo, who provided most of the samples used in the studies. I am also grateful to D.W. Blowes and R.G. Roberts of the University of Waterloo, and J.M. Bigham of The Ohio State University, for critical reading of the draft manuscript.

Chapter 4

Mineralogy of Ochre Deposits Formed by Sulfide Oxidation

Jerry M. Bigham
Department of Agronomy
2021 Coffey Road
The Ohio State University
Columbus, OH 43210-1086 USA

4.1. INTRODUCTION

The oxidative weathering of iron sulfide minerals commonly leads to the formation of ochreous precipitates that are part of a major water-pollution problem in regions with a history of mining for sulfide-bearing coal and ore deposits. Letterman and Mitsch (1978), for example, reported particulate deposition rates of up to 3 g/m2/day in a stream receiving acid coal-mine drainage. Such voluminous blankets of sediment not only have a ruinous impact on native fish populations and benthic communities, but also shorten the effective lifetimes of reservoirs, catchment basins, and wetlands constructed for treatment of acid mine drainage (Fennessy and Mitsch, 1989; Eger *et al.*, 1993; Hedin and Nairn, 1993). Similar accumulations of ochre have been shown to accompany the formation of acid sulfate soils, and to decrease the capacity of subsurface drainage lines installed for the purpose of soil aeration (Bloomfield, 1972; Süsser and Schwertmann, 1983).

Numerous studies have documented the role of mine-drainage ochres in the transport and attenuation of iron and trace elements in surface waters intercepting effluents from adits and waste dumps (*e.g.*, Chapman *et al.*, 1983; Johnson and Thornton, 1987; Filipek *et al.*, 1987; Winland *et al.*, 1991; Fuge *et al.*, 1994; Webster *et al.*, 1994). The natural tendency for these elements to partition into the solid phase through precipitation, sorption, and coprecipitation reactions may be regulated to cleanse wastewaters in commercial treatment systems (*e.g.*, Merrill *et al.*, 1986; Norton *et al.*, 1991); however, the compounds comprising mine-drainage ochres should not be viewed as inert phases under normal conditions. For example, recent studies have demonstrated that diurnal fluctuations in the chemistry of stream systems contaminated with mine drainage may be related to the cyclic dissolution and re-precipitation of ochre deposits caused by photochemically induced oxidation-reduction reactions

(McKnight *et al.*, 1988). Other, more dramatic spatial variations in the geochemical environment (*e.g.*, McKnight and Bencala, 1989; Kimball *et al.*, 1994) may also lead to transformations or changes in the solubilities of mineral phases comprising mine-drainage ochres.

Many quantitative geochemical models for predicting natural water composition are based on chemical equilibria between water and associated solid phases (Nordstrom *et al.*, 1990). Unfortunately, the mineralogy of ochreous precipitates from sulfate-rich mine waters has been oversimplified in most studies of mine drainage. Because of poor crystallinity, such precipitates are commonly referred to in technical articles simply as "amorphous" ferric hydroxide. While it is true that rapid oxidation and hydrolysis of iron may lead to the precipitation of compounds with extremely small particle size (≤10 nm), these materials still represent significant mineralogical diversity. The objectives of this paper are to 1) briefly discuss analytical techniques that have proven useful for the identification and characterization of poorly crystalline products of sulfide oxidation, 2) describe the known range of minerals associated with mine drainage ochres, 3) present a simple case study where analytical techniques and mineral properties can be demonstrated, and 4) summarize our current state of knowledge concerning biogeochemical factors that influence mineral speciation in sulfate-rich waters.

4.2. METHODOLOGY

4.2.1. Sample Collection and Handling

Ochre deposits produced by sulfide oxidation may occur as hardpans in waste dumps (McSweeney and Madison, 1988; Blowes *et al.*, 1991), as soft crusts associated with the seepage and overland flow of mine drainage (Bigham *et al.*, 1992), as sludge in containment/treatment ponds (Milnes *et al.*, 1992), and as loose suspensions of sediment in streams and ditches receiving sulfatic effluents (Karlsson *et al.*, 1988). Consolidated specimens may be relatively easy to secure for laboratory analysis, whereas loose sediments may require access to pumps and the collection of large volumes of material in order to ensure adequate sample size.

Proper treatment of samples following collection depends entirely upon the intended course of study. In all cases, drying at elevated temperatures should be avoided if mineralogical analyses are to be conducted. Drying under such conditions may produce irreversible changes due to the high surface area and poor crystallinity of many mine-drainage ochres. Air drying or freeze drying provide acceptable alternatives. Prior to drying, it may be desirable to remove excess soluble salts by centrifugation, filtration or rapid dialysis. Likewise, it may be possible to reduce or eliminate contamination from detrital mineral particles (*e.g.*, quartz) through the application of

sieve and/or gravity sedimentation techniques. Mineral suites should be simplified as much as possible because of the inherent difficulties involved in analyzing poorly crystalline materials.

4.2.2. Selective-dissolution Analysis

Selective-dissolution analysis is a destructive approach that usually includes a suite of chemical extractants designed to exploit the differential dissolution kinetics of minerals occurring in complex mixtures. Ideally, a given dissolution technique should be mineral-specific so that the phase in question is removed quantitatively while leaving other sample constituents unaltered. Strictly speaking, such a separation is impossible with most field samples because they either contain minerals with similar dissolution characteristics or with fairly wide ranges in crystallinity. Nevertheless, selective-dissolution techniques are simple, inexpensive, and may be fairly quantitative if the phases extracted can be verified by other methods of analysis.

Over the past several decades, soil scientists and geologists have developed a number of methods for the selective extraction of Fe oxides (Borggaard, 1988; Chao and Theobald, 1976). Perhaps the best known of these is the dithionite-citrate-bicarbonate (DCB) method of Mehra and Jackson (1960) which takes advantage of the sensitivity of these compounds to reductive dissolution. Numerous variations of this technique have since been proposed (*e.g.*, Coffin, 1963) and new approaches based on chemical reduction are still being developed (*e.g.*, Ryan and Gschwend, 1991). In general, methods utilizing reductive dissolution solubilize Fe occurring as oxides and oxyhydroxides, with minimal impact on other phases (*e.g.*, the silicates). Such methods are generally incapable of distinguishing between different oxide species (*e.g.*, goethite *vs.* hematite).

Methods designed to speciate minerals or phases within the iron oxide/oxyhydroxide group usually involve complexation and/or protonation reactions. In most instances, these methods target poorly crystalline phases and take advantage of naturally accelerated dissolution rates associated with structural disorder. For example, long-term (>90 days) extractions with weak, alkaline solutions of EDTA (a chelating agent) have been proposed for the selective dissolution of "amorphous" Fe oxides in mixed assemblage with silicates or crystalline Fe-oxides (Borggaard, 1982). A more rapid and widely utilized approach for achieving the same goal involves an acid medium with oxalate as the chelating agent. This method was originally proposed by Tamm (1922) and was later modified by Schwertmann (1964). As presently constituted, the technique requires a 2-to-4 hr extraction with 0.2 *M* ammonium oxalate at pH 3 in the dark. Although the sample-solution ratio is not particularly critical, the dissolution reaction is strongly catalyzed both by light (De Endredy, 1963) and by the presence of Fe^{2+} (Fischer, 1972). Thus, minerals such as magnetite and siderite are rapidly dissolved in acid ammonium oxalate (Rhoton *et al.*, 1981). Despite

these limitations, ratios of oxalate-to-dithionite-extractable iron (Fe_o/Fe_d) have been widely used to assess the relative crystallinity of secondary Fe(III) oxides produced by weathering reactions in a variety of surface environments, including mine-drainage systems (Brady *et al.*, 1986; Bigham *et al.*, 1990; Murad *et al.*, 1994).

4.2.3. X-ray and Differential X-ray Diffraction

With proper handling and preparation, well-crystallized minerals formed as a result of sulfide oxidation can commonly be identified readily by X-ray diffraction (XRD) using either Debye-Scherrer or diffractometer techniques. Conventional diffractometers are also useful for the identification of poorly crystallized phases, but analyses must be carried out by slow step-scanning with computer-assisted systems capable of digital data collection and peak-profile analysis. Relatively inexpensive commercial hardware and communications software packages are now available for automation of older XRD systems. X-ray sources yielding CoKα or FeKα radiation are desirable but are not required for analysis of Fe-rich phases so long as the system is equipped with a diffracted-beam monochromator.

The most difficult situations arise when a poorly crystallized phase(s) is present as a minor constituent (<25 wt%) in a sample that also contains well-crystallized components. In these instances, weakly resolved diffraction effects arising from the phase with short-range structural order tend to become "lost" in the background. This problem can be overcome, at least in part, by a combination of XRD and selective-dissolution analysis. Schulze (1981) demonstrated that if a step-scanned XRD pattern obtained from a sample after selective dissolution of all or part of the iron oxide minerals is subtracted from one obtained before extraction (*i.e.*, the original sample), a differential X-ray diffraction (DXRD) pattern of the dissolved fraction can be obtained. He found that goethite or hematite could be detected in a sample containing as little as 1.8 wt % DCB-soluble iron using the DXRD method. Schwertmann *et al.* (1982) subsequently reported that 15 wt % was about the lower limit of detection by DXRD for poorly crystallized ferrihydrite occurring in natural spring deposits and soil samples. The method has also been successfully employed to study the mineralogy of ochre deposits resulting from sulfide oxidation under both natural (Brady *et al.*, 1986) and laboratory conditions (Bhatti *et al.*, 1993).

4.2.4. Mössbauer Spectroscopy

The Mössbauer effect is a nuclear phenomenon involving the resonant absorption of γ-rays. For resonant absorption to occur, there must be limited recoil by both the emitting and absorbing atoms, and the nuclear environments in the source and absorber must be identical. If these environments differ, the energy of the γ-rays must be shifted accordingly, and this is usually accomplished by vibrating the source so as to create a Doppler effect. The Mössbauer isotope of interest in iron-bearing minerals is

^{57}Fe, which has a natural abundance of about 2.19 % (Bancroft, 1973).

In order to generate ^{57}Fe Mössbauer spectra, a ^{57}Co source is used. The ^{57}Co decays by electron capture to ^{57}Fe in an excited state which passes to the ground state with emission of a γ-ray having an energy of 14.41 keV (among others). This γ-ray is generally the most suitable for ^{57}Fe-Mössbauer spectroscopy because it has a low recoil energy and a narrow resonant line-width.

The utility of Mössbauer spectroscopy arises from three major factors. First, the Mössbauer spectrum of an iron mineral is characteristic of that mineral and, with proper interpretation, can be used as a "fingerprint." Secondly, ^{57}Fe-Mössbauer spectroscopy is specific for iron so that analyses may be conducted of iron-bearing compounds in low concentration and without spectral interference from other minerals. Finally, the Mössbauer effect is a nuclear phenomenon and can be used to study finely divided or poorly crystallized materials that may not be responsive to other analytical techniques requiring long-range structural order.

Three parameters, the isomer shift (δ), quadrupole splitting (ΔE_Q), and magnetic hyperfine field (B_i) are commonly extracted from the Mössbauer spectra of iron compounds. The numerical values of these parameters depend upon the type and magnitude of hyperfine interactions that exist between the charge distribution of ^{57}Fe nuclei and extranuclear electric and magnetic fields. Isomer-shift values for Fe^{2+} and Fe^{3+} usually fall within characteristic but separate ranges so that this parameter may be used to determine the oxidation state of iron in a compound. The quadrupole interaction arises when an electric field gradient is imposed on the nucleus resulting in a splitting of the nuclear energy levels and the appearance of a two-line Mössbauer spectrum. The magnitude of this splitting is sensitive to oxidation state, coordination number, and local site distortions. In some iron minerals, the nuclear energy levels of ^{57}Fe may be further split due to interactions with strong, internal magnetic fields. The result is a six-line spectrum wherein the magnitude of the splitting is proportional to the strength of the internal field. Most of the iron oxides are antiferromagnetic, which means that they yield a six-line Mössbauer spectrum because of an antiparallel alignment of equal magnetic moments below a characteristic temperature called the Néel point. Above this temperature, thermal fluctuations prevent the antiparallel alignment of magnetic moments associated with neighboring Fe(III) ions; the oxide behaves as though it is paramagnetic, and its Mössbauer spectrum consists of a doublet.

Additional information about the nuclear environment can be extracted from the Mössbauer line-widths and shapes. Line-widths exceeding about 0.3 mm s^{-1} and significant deviations from Lorentzian shape are indicative of complex conditions in the absorber (Murad, 1988). A good example is the nonideal behavior associated with the phenomenon of superparamagnetic relaxation. This phenomenon is common to small

(<50 nm) iron oxide particles, and is apparently caused by the disruptive effect of the particle surface on long-range magnetic order. Superparamagnetic relaxation averages out the net magnetic field above a certain blocking temperature characteristic of the mineral and the particle size. At or near this temperature, the typical six-line magnetic spectrum "relaxes" to a two-line Mössbauer spectrum characteristic of paramagnetic materials. Relaxation effects of this type can be counteracted by reducing the temperature of the absorber. Because the iron minerals comprising mine drainage ochres typically occur as microcrystals, it is important to utilize a Mössbauer spectrometer equipped with a cryostat so that analyses can be conducted at low temperatures (77 to 4 K).

4.2.5. *Other Methods of Analysis*

Mineralogical studies of mine-drainage ochres may be facilitated by many different methods of analysis, but several in addition to those already discussed should be mentioned.

a. Color

Perhaps the most striking feature of ochre deposits arising from sulfide oxidation is their bright, yellow-to-red coloration. Many mineralogists are wary of using color as a diagnostic property because of the well-known tendency for pigmentation to vary under the influence of such factors as particle size, aggregation, chemical composition, admixtures, *etc.* There is also a widespread misconception that the color of sediments and other "earthy" materials cannot be measured with any degree of confidence. In fact, the colors of such materials can be measured precisely in the laboratory using diffuse reflectance spectrophotometers (Torrent and Barrón, 1993), and portable tristimulus colorimeters are now available for equally precise determinations in the field (Post *et al.*, 1993). These technical advances, coupled with a better understanding of the spectral characteristics and genesis of minerals comprising ochre deposits (Schwertmann and Cornell, 1991; Schwertmann, 1993; Fanning *et al.*, 1993), should enable useful interpretations concerning not only mineralogy, but also local geochemical conditions to be derived from simple color measurements.

b. Infrared Spectroscopy

Infrared (IR) spectroscopy is a well-known resonance technique wherein spectra originate primarily from the vibrational stretching and bending modes within molecules. It is thus a powerful tool for the study not only of molecular structure, but also of ligand exchange reactions occurring at mineral surfaces. The IR spectrum of a mineral may provide a useful fingerprint for identification purposes, and IR spectroscopy has been the primary analytical tool employed in some studies of the ochreous products from sulfide oxidation (Lazaroff *et al.*, 1982, 1985). In these minerals, diagnostic absorption bands arise primarily from the presence of OH and SO_4 groups occurring in various configurations.

c. Electron Optical Techniques

Electron optical techniques find natural application in studies of the mineralogy and morphology of the colloidal products resulting from sulfide oxidation. Although particle morphology suffers from many of the same diagnostic uncertainties associated with color, it now seems clear that "typical" morphologies can be assigned to the minerals comprising most mine-drainage ochres. These crystal habits are best observed at the level of resolution afforded by the conventional transmission electron microscope (TEM) and are usually most clearly expressed in samples collected as loose precipitates. The consolidation and/or cementation of ochres into crusts and hardpans seems to have a negative impact on the expression of normal particle morphology. Consequently, morphological analyses of such materials should be viewed with caution. In such cases, selected-area electron diffraction and chemical analyses conducted with a scanning transmission electron microscope may be essential for particle identification.

4.3. MINERALS ASSOCIATED WITH MINE-DRAINAGE OCHRES

The information presented in this section is taken from the technical literature and from studies of specimens collected from an array of mine-drainage environments occurring at various geographic locations. These include mines operated for the production of bituminous coal, lignite, pyrite, silver, copper, and uranium. The aggregate of this information suggests that the major mineral phases associated with mine-drainage ochres include goethite, lepidocrocite, ferrihydrite, schwertmannite, and jarosite. A summary of the major properties of these minerals is presented in Table 4.1.

4.3.1. *Goethite α-FeOOH*

Goethite is usually considered to be the most stable form of Fe(III) oxide, and it occurs in almost every type of surface environment (Schwertmann and Taylor, 1989; Schwertmann and Fitzpatrick, 1992). In mine-drainage precipitates, goethite is commonly observed as a trace or minor constituent, but is rarely the dominant phase. These goethites have typical, yellowish brown colors with Munsell hues ranging between 7.5 YR and 10 YR. Whereas well-crystallized and/or synthetic goethites commonly display a fibrous or lath-like morphology, those occurring in mine-drainage precipitates usually form short, rod-like particles (Brady *et al.*, 1986, and Figure 4.1a). Typical XRD line-widths at half height are about 1o 2Θ for CoKα radiation (Figure 4.2), corresponding to a particle size of about 15 nm. In contrast to other goethite particles of similar dimensions, which exhibit little reactivity toward ammonium oxalate at pH 3.0, the mine-drainage specimens examined to date have shown moderate solubility in oxalate (Fe_o/Fe_d ratios on the order of 0.3). The reason for this enhanced reactivity is unknown.

Table 4.1. Properties† of minerals encountered in mine-drainage ochres

Mineral Name:	Goethite	Lepidocrocite	Ferrihydrite	Schwertmannite	Jarosite‡
Ideal Formula:	α-FeOOH	γ-FeOOH	~$Fe_5OH_8 \cdot 4H_2O$	$Fe_8O_8(OH)_8SO_4$	$KFe_3(OH)_6(SO_4)_2$
Crystal system	Orthorhombic	Orthorhombic	Trigonal	Tetragonal	Hexagonal
Cell dimensions (Å)	a = 4.608 b = 9.956 c = 3.022	a = 3.88 b = 12.54 c = 3.07	a = 5.08 c = 9.4	a = 10.66 c = 6.04	a = 7.29 c = 17.16
Color	Yellowish brown (7.5YR–10YR)	Orange (5YR–7.5YR)	Reddish brown (5YR–7.5YR)	Yellow (10YR–2.5Y)	Straw yellow (2.5Y–5Y)
Crystal shape	Short rods	Laths	Spherical	Pin-cushion	Pseudocubic
Crystallinity	Moderate	Moderate	Poor	Poor	Good
Most intense XRD spacings (Å)	4.18, 2.45 2.69	6.26, 3.29, 2.47, 1.937	2.54, 2.24, 1.97, 1.73, 1.47	4.86, 3.39, 2.55, 2.28, 1.66, 1.51	5.09, 3.11, 3.08
Major IR bands (cm^{-1})	890, 797	1161, 1026, 753	Nil	1175, 1125, 1055 975, 680, 615	1181, 1080, 1003 628, 493, 472
Néel temp. (K)	400	77	28–115§	75	55–60
Magnetic hyperfine field (T) at:					
295K	38.2	—	—	—	—
77K	50.0	—	≤ 45.1	—	—
4.2K	50.6	46.0	46.5–50.0	45.4	47.0

† Data taken from
Bigham et al. (1990) — Murad (1988)
Bigham et al. (1992) — Murad et al. (1988) — Schwertmann & Fitzpatrick (1992)
Doner & Lynn (1989) — Murad et al. (1994) — Schwertmann & Taylor (1989)
Fanning et al. (1993) — Powers et al. (1975) — Takano et al. (1968)

‡ Properties listed are specific to jarosite, but natrojarosite and hydronium jarosite may also occur.

§ Blocking temperature.

Table 4.1. Properties of minerals encountered in mine-drainage ochres.

Well-crystallized specimens of goethite have a Néel temperature of about 400 K and yield a six-line Mössbauer spectrum at room temperature (Table 4.1). By contrast, room-temperature spectra from mine-drainage goethite consists of a doublet, indicating superparamagnetic relaxation that is probably a result of small particle size. At 4.2 K these same goethite samples are magnetically ordered, but they yield hyperfine fields that are slightly smaller than those typical of bulk specimens, thus once again indicating reduced particle dimensions (Murad *et al.*, 1994). Infrared spectra of mine-drainage goethite show diagnostic bands due to OH bending at 890 and 797 cm^{-1}, but may also exhibit additional features arising from surface adsorption of SO_4 (Brady *et al.*, 1986).

4.3.2. *Lepidocrocite γ-FeOOH*

Lepidocrocite is a polymorph of goethite that is commonly recognizable in the field by bright orange colors having Munsell hues in the 5 YR to 7.5 YR range, chromas of 6 to 8, and values ≥6 (Schwertmann, 1993). Although lepidocrocite is widespread in surface environments, particularly in soils and recent sediments, observations of the mineral as a product of sulfide weathering are limited. Romberg (1969) reported lepidocrocite as a pseudomorphic replacement product of pyrite; Blowes *et al.* (1991) identified lepidocrocite as a cementing agent in hardpans formed at the depth of active oxidation in sulfide mine tailings, and additional similar occurrences are reported by Jambor (this Volume). Milnes *et al.* (1992) detected poorly crystallized lepidocrocite in an ochreous sludge collected from a retention pond associated with a uranium mine in Australia, and Mann *et al.* (1992) used selected-area electron diffraction to identify microcrystalline lepidocrocite precipitated on the surfaces of microorganisms extracted from waters draining uranium tailings in the Elliot Lake district of Ontario, Canada. Although published XRD and electron optical data are consistent with the data summarized in Table 4.1, little is known about other properties of lepidocrocites from mine-drainage environments.

4.3.3. *Ferrihydrite ≈ $Fe_5OH_8.4H_2O$*

Ferrihydrite has become a popular but often misused synonym for "amorphous" ferric hydroxide. Consequently, it is not surprising to find many references to this mineral in the mine drainage literature (*e.g.*, Nordstrom, 1982a; Filipek *et al.*, 1987; Ferris *et al.*, 1989; Milnes *et al.*, 1992). Ferrihydrite has attracted the attention of physical as well as biological scientists, and its genesis and properties have been the subject of considerable research activity over the past two decades. Much of the resulting literature has been summarized in two recent review articles (Eggleton and Fitzpatrick, 1988; Childs, 1992).

Ferrihydrite occurring in soils and sediments has a rusty, reddish-brown color with Munsell hues in the 5 YR to 7.5 YR range and Munsell values <6 (Schwertmann,

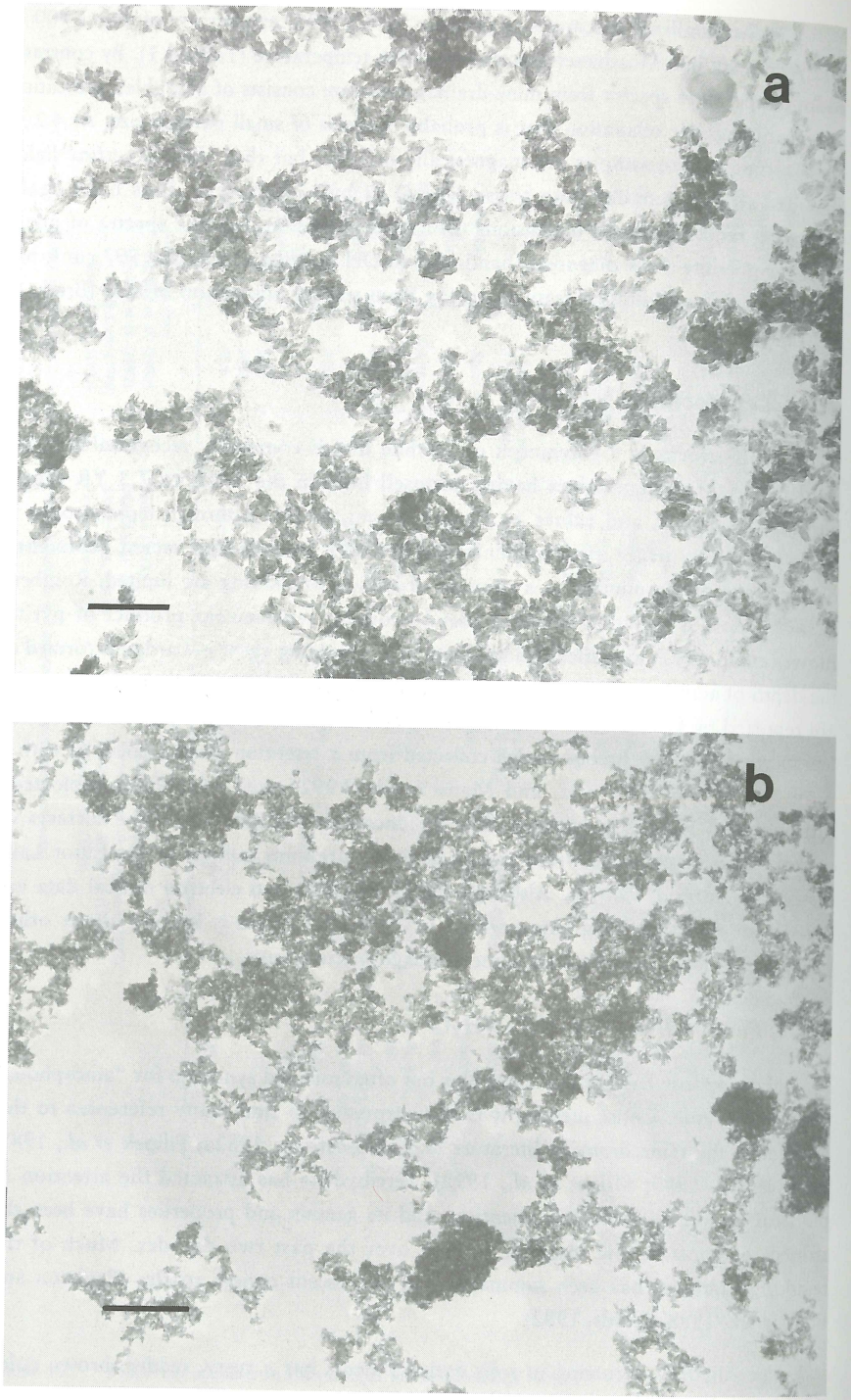

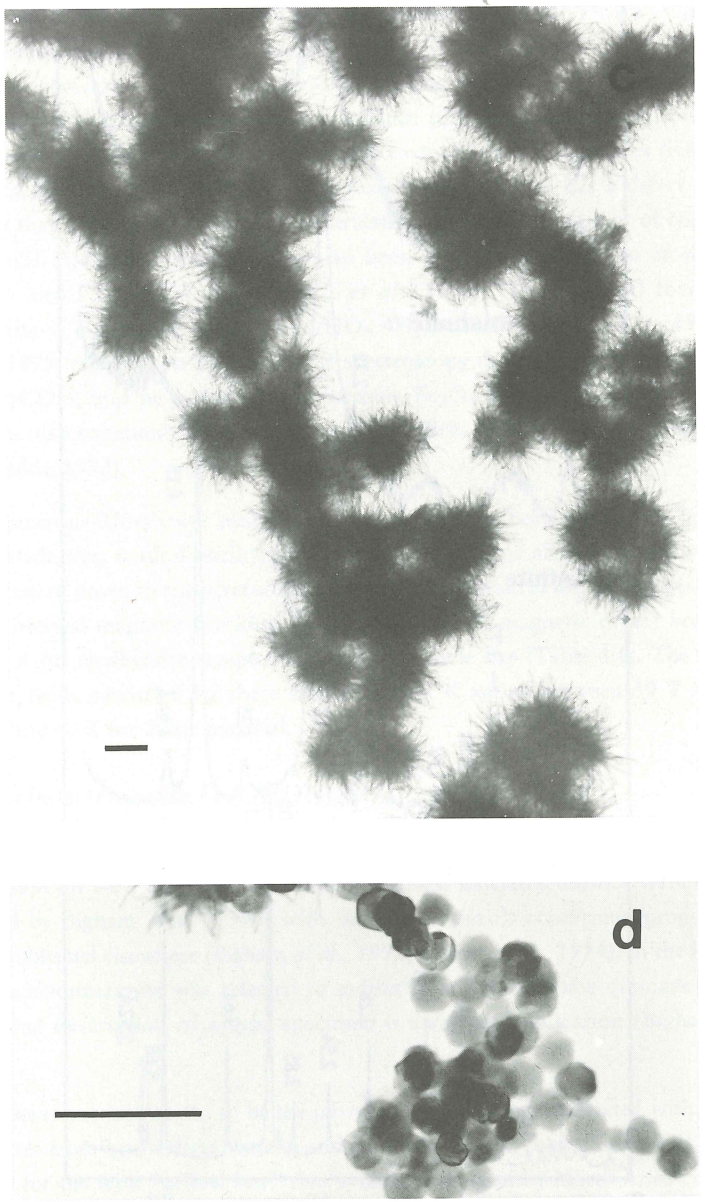

Figure 4.1. Transmission electron micrographs of minerals occurring in mine-drainage ochres: (a) goethite, (b) ferrihydrite, (c) schwertmannite, and (d) jarosite. Scale bar = 0.2 μm.

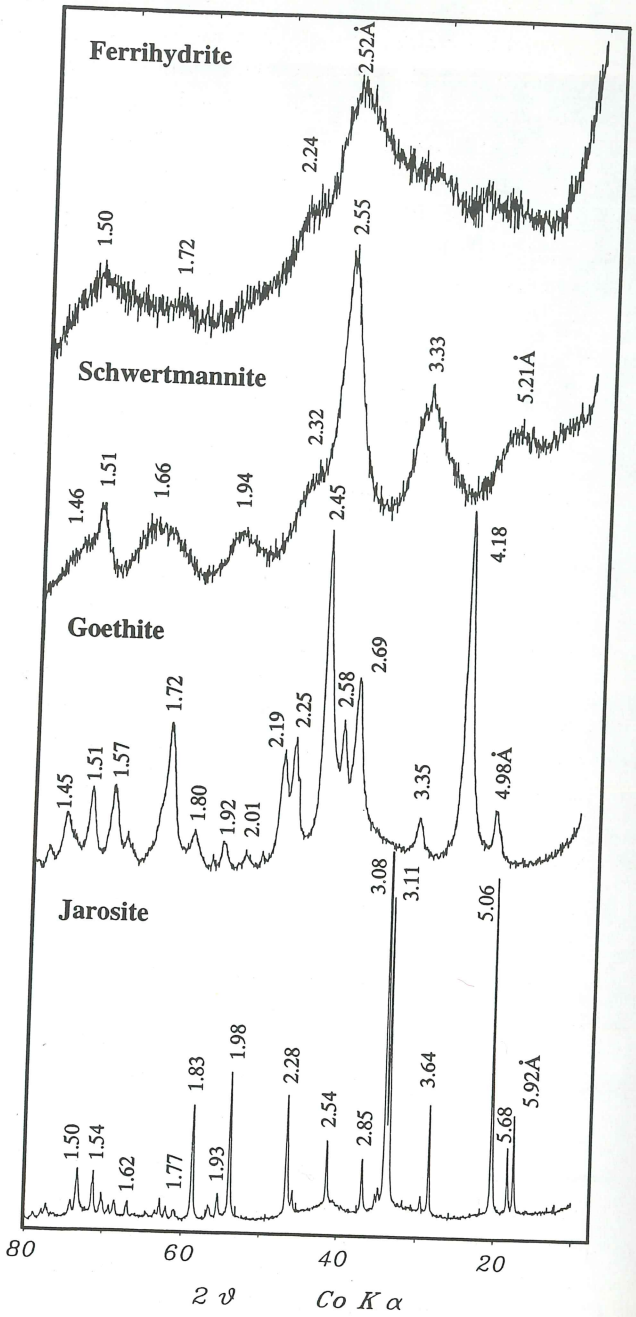

Figure 4.2. Representative X-ray diffraction traces from minerals occurring in mine-drainage ochres (modified from Bigham *et al.*, 1992).

1993). Natural and synthetic samples both usually consist of highly aggregated, spherical particles with diameters in the order of 2 to 6 nm (Figure 4.1b). Consequently, the mineral has high specific surface areas in the range of 200 to 600 m^2/g, and it is readily soluble in both acid ammonium oxalate and DCB so that $Fe_o/Fe_d \cong 1$. Ferrihydrite is always poorly crystallized, but it can display a range of structural order that gives rise to XRD patterns consisting of anywhere from two (worst crystallized) to six (best crystallized) broad bands (Carlson and Schwertmann, 1981). Most mine-drainage ferrihydrite samples yield two- to four-band profiles (Figure 4.2). Towe and Bradley (1967) originally proposed that ferrihydrite has a defect structure based on that of hematite; however, the structure has remained a point of controversy and several alternative models have also been developed (Harrison *et al.*, 1967; Eggleton and Fitzpatrick, 1988; Drits *et al.*, 1993). The nominal formula for ferrihydrite is commonly taken as $Fe_5HO_8.4H_2O$ (Towe and Bradley, 1967), but Russell (1979) reported on the basis of IR spectroscopy that about half the hydrogen is present as OH, and he suggested the formula $Fe_2O_3.2FeO(OH).2.5H_2O$. Natural specimens also commonly contain up to about 9 wt% Si (Carlson and Schwertmann, 1981; Childs, 1992).

Numerous Mössbauer analyses of ferrihydrite have been conducted. Because of small particle size, natural ferrihydrite is superparamagnetic at room temperature and may remain so down to temperatures as low as 23 K (Murad *et al.*, 1994). Murad *et al.* (1988) observed magnetic blocking temperatures (50 % magnetic order) between 28 and 115 K for ferrihydrite samples of different particle size (Table 4.1). The magnetic hyperfine fields measured for these samples at 4.2 K varied between 50 T for 6-line material and 47 T for 2-line material.

4.3.4. *Schwertmannite* $Fe_8O_8(OH)_6SO_4$

Schwertmannite is a new mineral that has only recently been approved by the Commission on New Minerals and Mineral Names. Its characteristics were originally described by Bigham *et al.* (1990) with subsequent details concerning properties and genesis published elsewhere (Bigham *et al.*, 1992; Murad *et al.*, 1994). In the latter two papers, schwertmannite was referred to indirectly as MDM (mine drainage mineral). The formal description of a type specimen is awaiting publication (Bigham *et al.*, 1994).

Schwertmannite seems to be the most common mineral associated with ochreous precipitates from acid sulfate waters, and its bright yellow color (Table 4.1) probably accounts for the term "yellow boy" that is commonly used by North American miners in reference to acid mine drainage. Like ferrihydrite, schwertmannite is a very poorly crystallized mineral characterized by high specific surface area (100 to 200 m^2/g) and rapid solubility in acid ammonium oxalate. The former is consistent with a unique, "pin-cushion" morphology that is readily observed in particles isolated from loose

precipitates (Figure 4.1c).

Schwertmannite is also easily distinguished from ferrihydrite and other associated minerals by its XRD profile, which consists of eight broad bands for d >1.4 Å (Figure 4.2). Comparisons of this profile with those of synthetic specimens prepared under different geochemical conditions led Bigham *et al.* (1990) to conclude that schwertmannite has a tunnel stucture similar to that of akaganéite, ß-$FeO(OH)_{1-x}Cl_x$ (nominally ß-FeOOH), with SO_4 assuming the position of Cl in the tunnel cavities. The presence of SO_4 is readily confirmed both by infrared spectroscopy (Table 4.1) and by chemical analysis. Natural specimens of schwertmannite contain 10 to 15 wt% SO_4, which translates to an Fe/S mole ratio ranging from 5 to 8 and a structural formula varying between $Fe_8O_8(OH)_6SO_4$ and $Fe_8O_8(OH)_{4.8}(SO_4)_{1.6}$.

Mössbauer data have shown the Fe in schwertmannite to be exclusively trivalent and in octahedral coordination (Murad *et al.*, 1990). The mineral has a Néel temperature of 75 ± 5 K and a saturation magnetic hyperfine field of about 45.5 T at 4.2 K. The former is lower than the Néel temperature of any iron oxide, and the latter is lower by about 1.5 T than those of even the most poorly crystallized ferrihydrites (Table 4.1). The Mössbauer spectra of both paramagnetic and magnetically ordered schwertmannite are asymmetric, indicating multiple environments for Fe^{3+} that presumably arise from the incorporation of SO_4 into the structure. Sulfate probably also inhibits magnetic exchange interactions between neighboring iron atoms and is thereby responsible for the low magnetic ordering temperature and hyperfine field.

4.3.5. *Jarosite $KFe_3(OH)_6(SO_4)_2$*

Jarosite is a common mineral in acid, high-sulfate environments, usually appearing as straw-colored (Munsell hue of 2.5 Y or yellower and chroma >6) mottles and efflorescences within the saturated or vadose zones of mine tailings and acid sulfate soils (Fanning *et al.*, 1993). Jarosite has often been implicated as an important phase in fresh precipitates from surface waters carrying mine drainage (*e.g.*, Nordstrom, 1982a; Karathanasis *et al.*, 1988), but its importance in this regard has probably been overestimated. Compared with other minerals occurring in mine-drainage ochres, jarosite is usually well-crystallized and easily identified from its characteristic XRD pattern (Figure 4.2). Pseudocubic crystals are commonly observed under the electron microscope (Figure 4.1d), but tabular (Doner and Lynn, 1989) and botryoidal forms (Lazaroff *et al.*, 1985) have also been reported. Mössbauer and magnetic studies (Takano *et al.*, 1968; Afanasev *et al.*, 1974; Powers *et al.*, 1975) have confirmed that jarosite is antiferromagnetic, with a Néel temperature of approximately 55 K, which is lower than those of schwertmannite or any of the iron oxides common to mine drainage (Table 4.1).

Jarosite is the most common member of a family of basic iron sulfates that may

arise by partial replacement or complete substitution of K^+ with other monovalent and some divalent cations. Natrojarosite has been reported to be fairly common in some acid sulfate soils (Ross *et al.*, 1982), and Chapman *et al.* (1983) identified both K and Pb varieties in mine drainage precipitates. Most studies of field samples have lacked sufficient detail to distinguish between species even though investigations of synthetic specimens (*e.g.*, Dutrizac and Kaiman, 1976; Leclerc, 1980) have revealed systematic variations in many diagnostic parameters within the jarosite family of compounds.

4.4. A CASE STUDY OF MINE-DRAINAGE PRECIPITATES IN OGG CREEK, OHIO

Southeastern Ohio sits on the northwest flank of the eastern U.S. coal province. Coal-bearing rocks in this region are of Pennsylvanian and Permian age and yield bitumunious coals with medium (1.1—3.0 %) to high (>3.0 %) sulfur contents. Coal has been extracted in this area since the beginning of the 19th century using both underground and surface mining techniques. The former involved primarily drift mines, many of which have now flooded and become permanent sources of mine drainage. One of the most heavily polluted districts in the state is drained by Moxahala Creek, which is tributary to the Muskingum River. The primary source of coal in this area is the Middle Kittanning (#6) seam, with an average thickness of 1.5 to 2.0 m. Mining continues to the present, but the greatest activity occurred from 1930 through 1960.

From March, 1981, to August, 1982, water and sediment samples were collected from a small, 74.3-km^2 watershed within the Moxahala Basin (39°43'21" N. Lat.; 82°03'42" W. Long.). The watershed, consisting of Black Fork Creek, Ogg Creek, and Bennett Run (Figure 4.3) has experienced both surface and deep mine activity. The latter mines are now abandoned and are the primary source of mine-drainage pollution. Although the sampling in this study was not intensive and did not include basic discharge measurements, the results give a useful snapshot of the local geochemical environment. In addition, fairly detailed analyses of ochreous precipitates collected from the stream beds provide a means of demonstrating the analytical procedures discussed in Section 4.2.

4.4.1. *Materials and Methods*

Water samples were collected during periods of low stream flow from six sites as shown in Figure 4.3. Sites 1 and 2 represent reference areas upstream from major sources of pollution on Ogg Creek and Bennett Run. Effluent discharged from a buried adit at site 3 was the primary source of pollution in the study area. At its source, the drainage was clear but was in contact with abundant bacterial streamers (Johnson *et al.* 1979). Site 4 was immediately downstream from the entry of this drainage into Bennett Run and was also influenced by approximately 16 ha of unvegetated mine tailings in

the surrounding area. Sites 5 and 6 were located just below and approximately 1 km downstream from the confluence of Bennett Run and Ogg Creek.

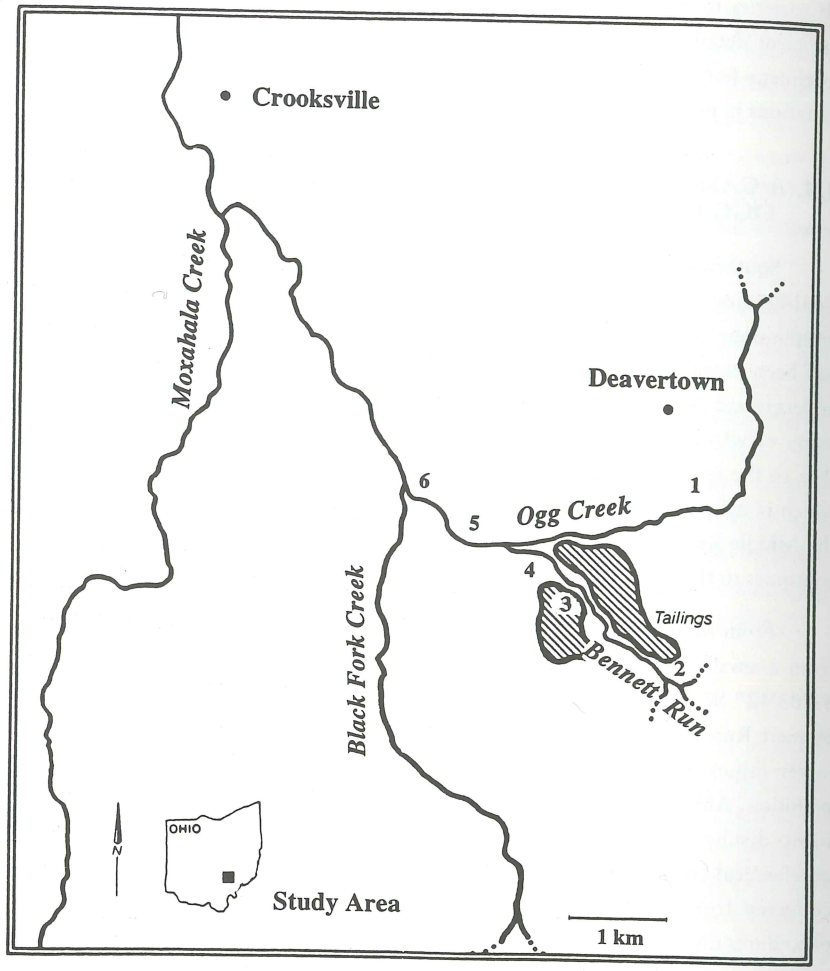

Figure 4.3. Location map for Ogg Creek and Bennett Run.

Three, 500-mL samples of solution were collected from each site during August, 1982. These samples were placed in foil-wrapped, polyurethane bottles, and were transported under ice to the laboratory, whereupon portions were warmed to room temperature and immediately analyzed for pH and Eh. Additional subsamples were filtered through 0.1-μm membranes, and aliquots were immediately analyzed for Fe(II) and total dissolved iron using a procedure modified from that of Stucki (1981). The remaining filtrates were acidified with 2 mL of ultrapure HNO_3 per 125 mL sample

and eventually were analyzed for Al, Ca, Mg, Mn, Na and trace metals by using inductively coupled plasma-emission spectroscopy (ICP). Sulfate in the filtrates was determined by using a standard, turbidimetric method. Finally, total Fe in aliquots of the original (unfiltered) samples was determined according to the method of Stucki (1981) following the addition of a chemical reductant. Percent colloidal Fe was calculated as the difference between total Fe in the unfiltered samples and total Fe passing the 0.1-μm membranes.

In addition to water samples, approximately 60 L of suspension containing a voluminous, yellow preciptate were collected from the stream bed at sites 4 and 5 by using a hand-held pump. In each case, the suspension was allowed to settle, and the supernatant liquid was decanted. The solid phase was then concentrated by centrifugation, washed by dialysis, quick-frozen, and freeze-dried. Both precipitates were analyzed by XRD and selective dissolution, and that from site 5 was further evaluated by Mössbauer, TEM, and other procedures described in detail elsewhere (Brady *et al.*, 1986; Murad *et al.*, 1994).

4.4.2. *Water Chemistry*

Water samples collected from sites 1 and 2 above the area of acid discharge contained background levels of common cations and yielded pH/Eh values typical of streams in the region with normal biological activity (Table 4.2). By contrast, the effluent draining the mine adit at site 3 was acidic and contained high concentrations of Fe, Al, and SO_4. Particulate Fe contents were low, and 95 % of the total dissolved Fe was in the form of Fe(II). Dilution coupled with rapid oxidation, hydrolysis, and precipitation of Fe occurred upon entry of the effluent into Bennett run, as is evident from the data for site 4 (Tables 4.2 and 4.3) and the immediate formation of cloudy, orangish yellow water in the field. This trend was accelerated at site 5 below the confluence with Ogg Creek. At this point, the total dissolved Fe content was one-tenth that of the original effluent, the proportion of Fe(II) had decreased to 0.59, and the content of colloidal Fe had increased to 49% of the total measured. Within an additional kilometer (site 6), the oxidation of Fe was nearly complete, and a decrease in colloidal Fe content suggested that most of the ochreous precipitate had settled to the stream bottom. The modest increase in pH from 2.9 to 3.2 downstream from the mine adit reflects the fact that sandstones and shales are the predominant rock types in the watershed. Consequently, surface waters are not highly buffered.

4.4.3. *Mineralogy*

a. Site 4

An XRD tracing from a random powder mount of the precipitate at site 4 is presented in Figure 4.4. All eight diffraction bands typical of schwertmannite are

Table 4.2. Chemical parameters for waters from Ogg Creek and Bennett Run — August, 1982

Site No.	pH	Eh	SO_4	Al	Ca	Fe	Mg	Mn	Na
		Volts	---------- mg/L ----------						
1	7.3	0.314	31	<1	43	<1	10	<1	18
2	6.8	0.320	32	<1	42	<1	10	<1	20
3	2.9	0.584	4543	343	80	1172	46	4	19
4	2.9	0.646	2000	154	80	273	37	5	31
5	3.1	0.659	1020	87	76	138	26	3	24
6	3.2	0.711	920	74	83	88	27	4	22

Table 4.3. Speciation of iron* in waters from Ogg Creek and Bennett Run — August, 1982

Site No.	Fe (II)	Fe(d)	Fe(t)	Fe(II)/Fe(d)	Colloidal Fe
	---------- mg/L ----------				%
3	1118	1172	1245	0.95	6
4	199	273	329	0.73	17
5	82	138	271	0.59	49
6	9	88	117	0.10	25

* Fe(II) = ferrous iron; Fe(d) = total "dissolved" iron passing a 0.1μm filter; Fe(t) = total iron;

$$\% \text{ Colloidal Fe} = \frac{\text{Fe(t)} - \text{Fe(d)}}{\text{Fe(t)}} \times 100$$

present (see Figure 4.2). In addition, sharp peaks due to the presence of 10.5 wt% detrital minerals (mostly quartz, feldspars, and kaolinite) are clearly expressed. Extraction of the sample with acid ammonium oxalate and DCB yielded 40.5% Fe_o, 40.7% Fe_d, and an Fe_o/Fe_d ratio of 0.99. The total SO_4 content was 13.9%. When these data are corrected for the detrital mineral content of the sample, the results are within the characteristic compositional range for schwertmannite. Consequently, the local geochemical conditions (pH = 2.9; $[SO_4]$ = 2000 mg/L; abundant Fe subject to rapid oxidation and hydrolysis) must be viewed as conducive to the formation of this mineral.

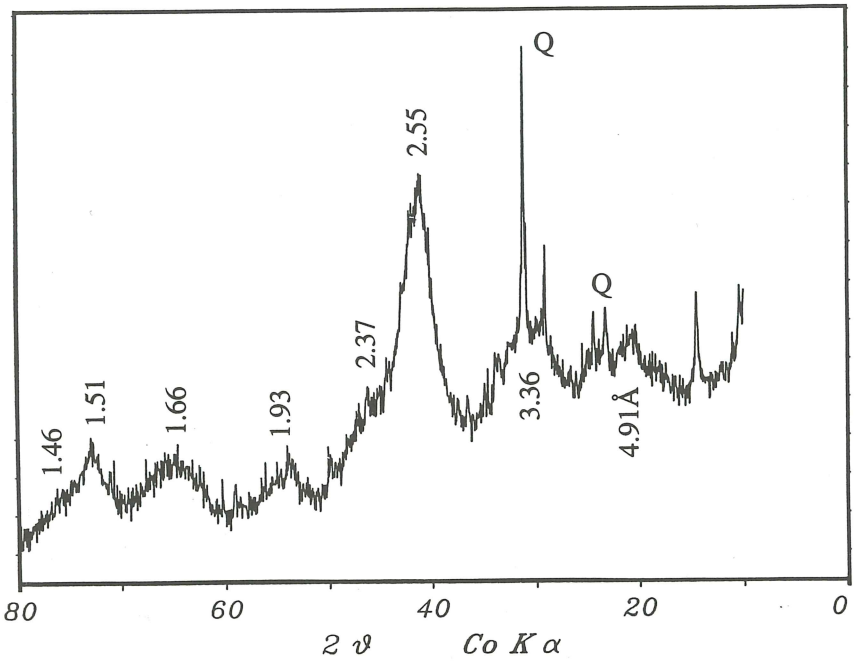

Figure 4.4. X-ray diffraction pattern from precipitate at Site 4.

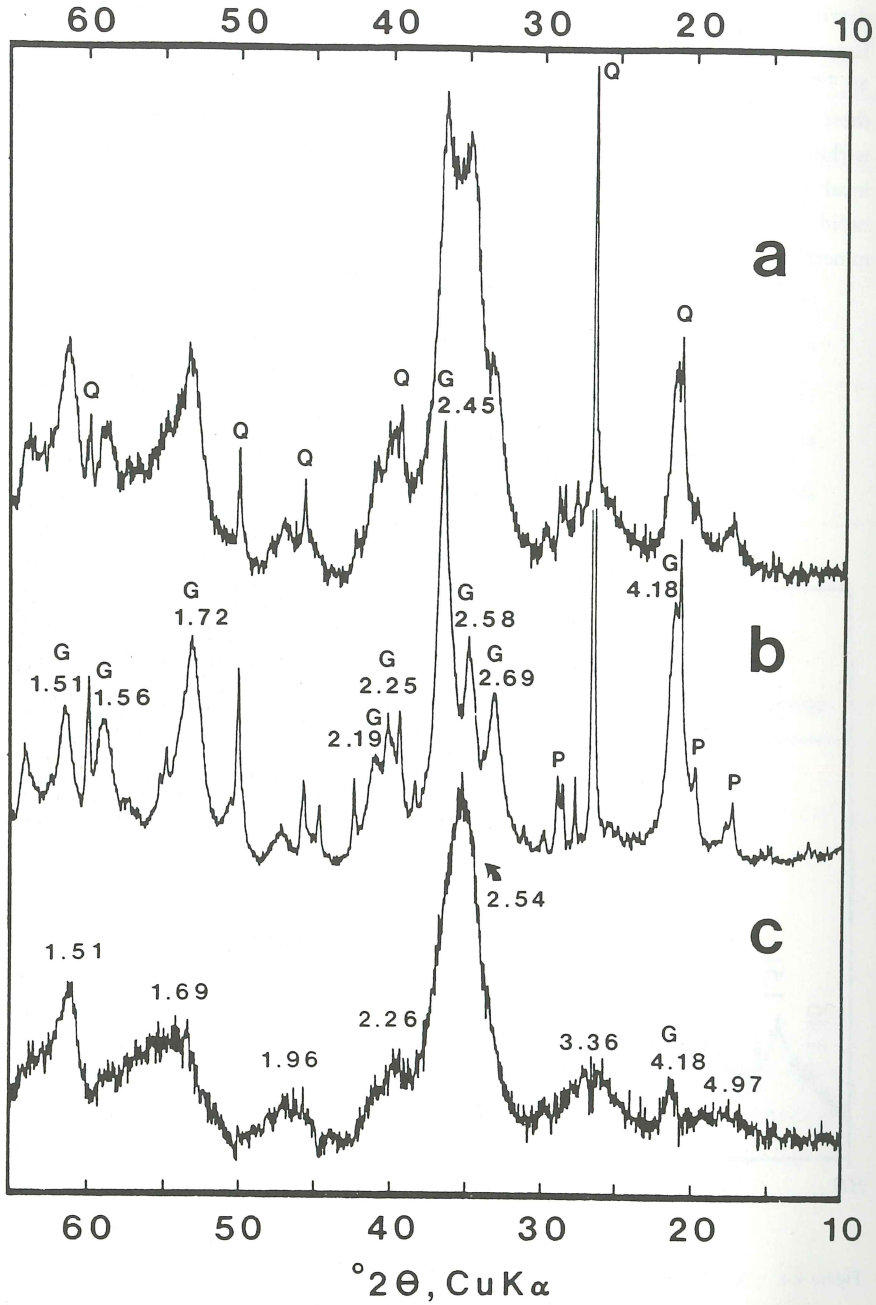

Figure 4.5. X-ray diffraction patterns from precipitate at Site 5: (a) untreated, (b) following 15-min oxalate extraction, (c) after subraction of (b) from (a) (DXRD). G = goethite, Q = quartz, P = phyllosilicates (from Brady *et al.*, 1986).

b. Site 5

The XRD tracing from the precipitate collected at site 5 (Figure 4.5a) is considerably more complicated than that from site 4, indicating that further dilution of the acid mine-effluent with fresh water from Ogg Creek has produced a material with mixed mineralogy. A TEM micrograph of the specimen shows particles with the characteristic "pin-cushion" morphology of schwertmannite together with short, rod-like particles of goethite (Figure 4.6).

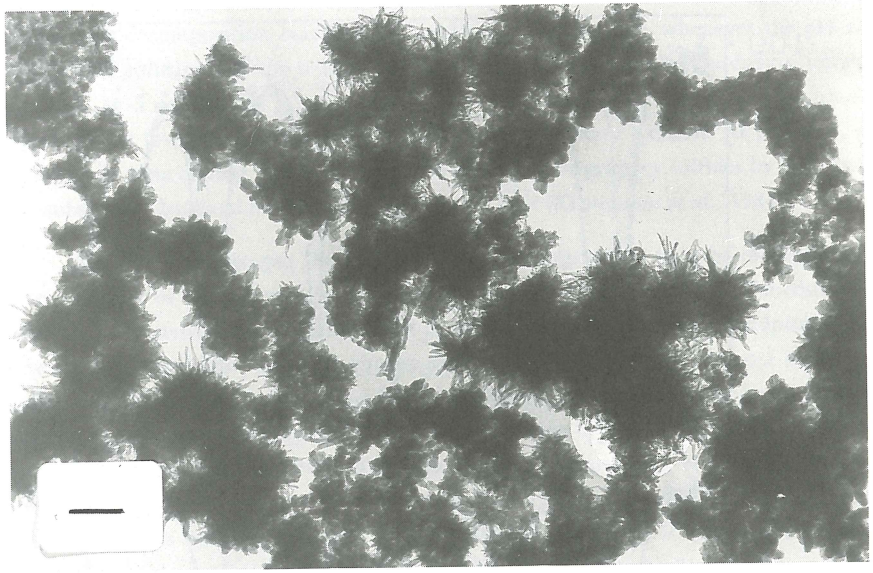

Figure 4.6. Transmission electron micrograph of precipitate at Site 5. Scale bar = 0.2 μm.

To further evaluate the presence of goethite, a subsample of the precipitate was subjected to a rapid, 15-min extraction with acid ammonium oxalate. This treatment removed 78% of the total, DCB-soluble Fe and left a residue consisting of quartz, phyllosilicates, and poorly crystallized goethite (Figure 4.5b). Diffraction effects from the oxalate-soluble component were observed by subtracting the data in Figure 4.5b from that in Figure 4.5a using the technigue of Schulze (1981). The resulting DXRD pattern (Figure 4.5c) is that of schwertmannite with a small contribution from dissolved goethite.

A Mössbauer analysis of the natural (untreated) specimen at 4.2 K (Figure 4.7a) confirms the presence of goethite and schwertmannite. The spectrum consists of two sextets, and a central doublet that is presumably a product of Fe^{3+} in detrital clay minerals. The inner sextet is associated with an average hyperfine field of 45.4 T and arises from schwertmannite. The outer sextet has a magnetic hyperfine field of 49.96 T

and is due to goethite. After a 2-hour oxalate treatment, the inner sextet disappears, leaving only the goethite spectrum and an enhanced paramagnetic doublet (Figure 4.7b). In a paragenetic sense, it is unknown whether the goethite in this sample has formed as a direct preciptate from the contaminated waters of Ogg Creek or is an alteration product of schwertmannite.

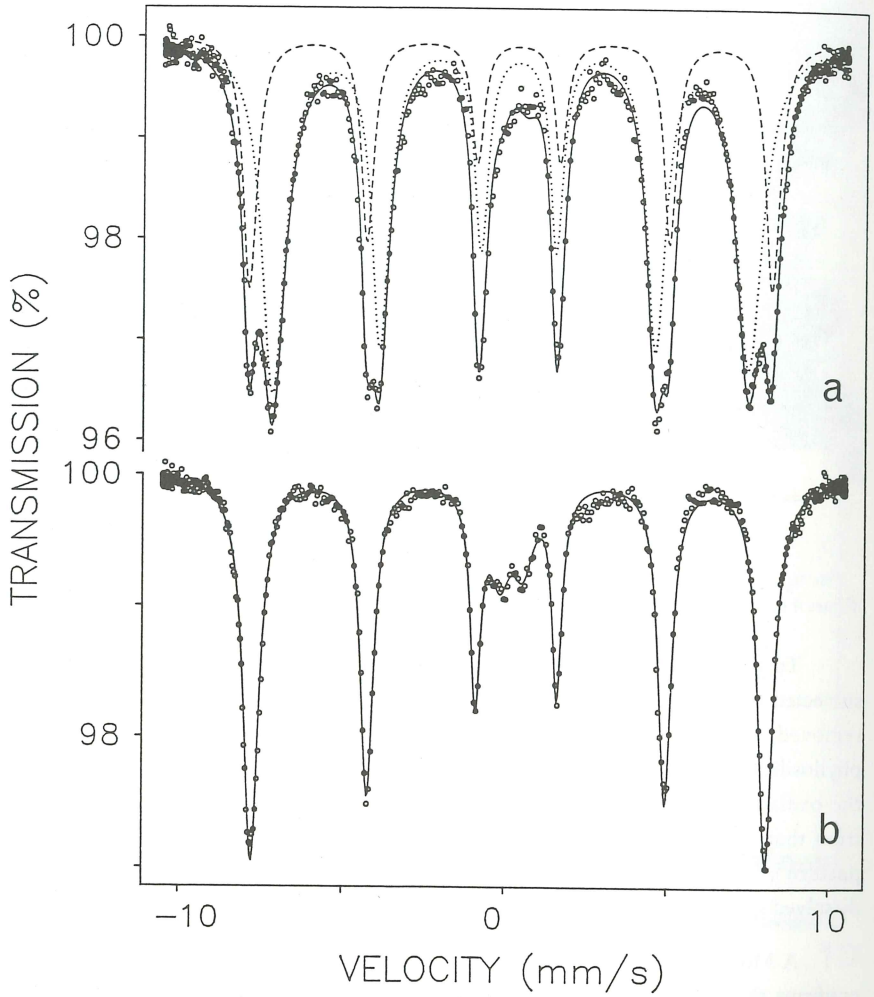

Figure 4.7. Mössbauer spectra taken at 4.2 K of precipitate at Site 5: (a) untreated and (b) following a 2-hour oxalate extraction. Subspectra in the untreated sample are for goethite (broken line) and schwertmannite (dotted line) (from Murad *et al.*, 1994).

4.5. BIOGEOCHEMICAL FACTORS INFLUENCING MINERAL SPECIATION IN OCHRE DEPOSITS

4.5.1. The Role of Bacteria

The important role played by acidophilic bacteria, such as *Thiobacillus ferrooxidans*, in the aqueous oxidation of pyrite and related minerals is now widely recognized (*e.g.*, Nordstrom, 1982a). Some controversy remains regarding the ability of bacteria in direct contact with sulfide grain surfaces to initiate the oxidation process through enzymatic pathways, but there is clear evidence that bacteria indirectly catalyze subsequent decomposition reactions by oxidizing aqueous Fe^{2+} whenever the pH of interstitial solutions drops below 4.5. The importance of rapid oxidation under strongly acid conditions is related to the fact that the activity of Fe^{3+} becomes significant at low pH, so that Fe^{3+} replaces O_2 as a primary oxidant. At pH <2.5, a near-steady-state cycling of Fe occurs via the oxidation of primary sulfides by Fe^{3+} and the subsequent bacterial oxidation of regenerated Fe^{2+} (Kleinmann *et al.*, 1981).

Any Fe^{2+} that escapes the cycle of pyrite decomposition may be incorporated into a variety of secondary minerals having a wide array of properties (Nordstrom, 1982a). Ultimately, however, most Fe^{2+} is oxidized, hydrolyzed, and precipitated as one of the "insoluble" mineral phases described in Section 4.3. Almost since its isolation, *Thiobacillus ferrooxidans* has been thought to accelerate the formation of ochreous precipitates associated with acid mine drainage by catalyzing the oxidation of iron (Colmer and Hinkle, 1947). Although Fe-encrusted bacterial remains have been isolated from mine-drainage sediments (Ferris *et al.*, 1989; Mann *et al.*, 1992; Milnes *et al.*, 1992), it is unlikely that the type of mineral produced is controlled by the physiology of the organism. The oxidation of Fe may be biologically induced, and the rate of oxidation may be under metabolic control, but the mineralization process itself is extracellular (Lowenstam and Weiner, 1989). In other words, geochemical parameters such as pH, $[SO_4]$, and $[HCO_3]$ determine the mineralogical fate of Fe once it is oxidized either by biotic or abiotic mechanisms.

4.5.2. Proton Activity

Pyrite decomposition is a complicated process involving several reactions that are proton-generating. Consequently, sulfatic mine drainage is usually assumed to be acidic. In fact, the pH of mine drainage may range from less than 2 to as high as 8.5 depending on the stage of the reaction and the geologic setting (Mills, 1985). Bigham *et al.* (1992) studied the mineralogical composition of ochres precipitated from a variety of mine effluents with pH in the range of 2.6 to 7.8 (Figure 4.8). Although they found that goethite occurred over the full range of effluent pH, it was the primary component in only two samples, both of which were formed from solutions with pH >6.0. Slightly acid to alkaline conditions also favored the formation of ferrihydrite, and these results

suggest that ferrihydrite may be more limited in distribution than previously indicated in the mine-drainage literature. A similar conclusion may be reached with regard to jarosite, which was detected in only a few sediments produced under the most acid (pH <3.3) conditions encountered. Brown (1971) has also noted that the solution pH should not exceed 3.0 if jarosite is to remain a stable phase. The most common mineral identified by Bigham *et al.* (1992) was schwertmannite. Schwertmannite was present in more than 60% of the specimens analyzed, and was particularly abundant in precipitates formed from "typical" mine effluents having pH values in the range of 3.0 to 4.0.

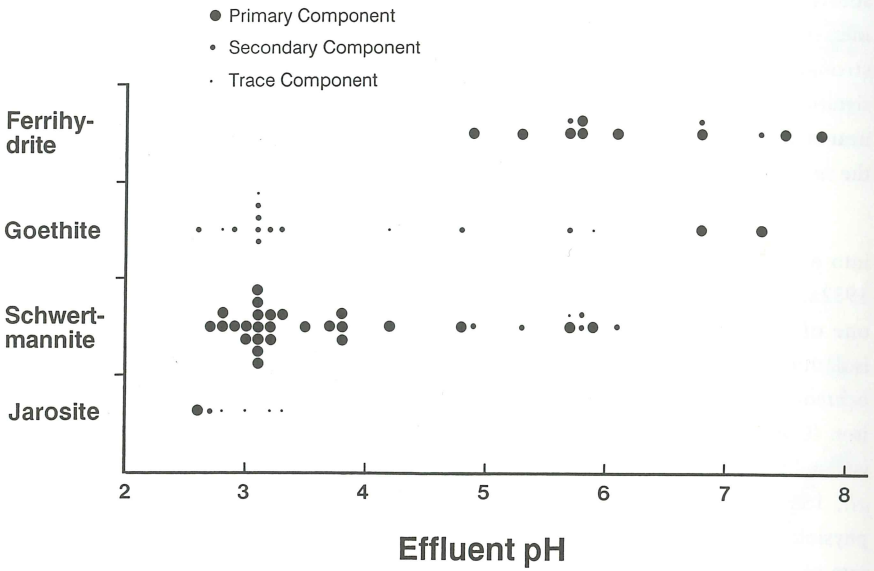

Figure 4.8. Distribution of mine-drainage minerals as a function of effluent pH (modified from Bigham *et al.*, 1992).

4.5.3. Dissolved Sulfate

Sulfate is obviously the most common anion associated with mine-drainage environments, and it is reasonable to expect that the activity of sulfate in solution plays a major role in defining pathways of mineral speciation during ochre formation. Jarosite-type compounds, for example, are easily synthesized from acid solutions containing excess sulfate and suitable concentrations of metal cations (Fe, K, Na, *etc.*) by using either abiotic (Brown, 1970; Dutrizac, 1984) or biotic (Ross *et al.*, 1982; Lazaroff *et al.*, 1982; Grishin *et al.*, 1988) approaches. Critical conditions for the formation of jarosite can also be calculated from available thermodynamic data (*e.g.*, Brown, 1971; Vlek *et al.*, 1974); however, it is not altogether clear what level of sulfate activity is actually required to form jarosite under field conditions. In results reported

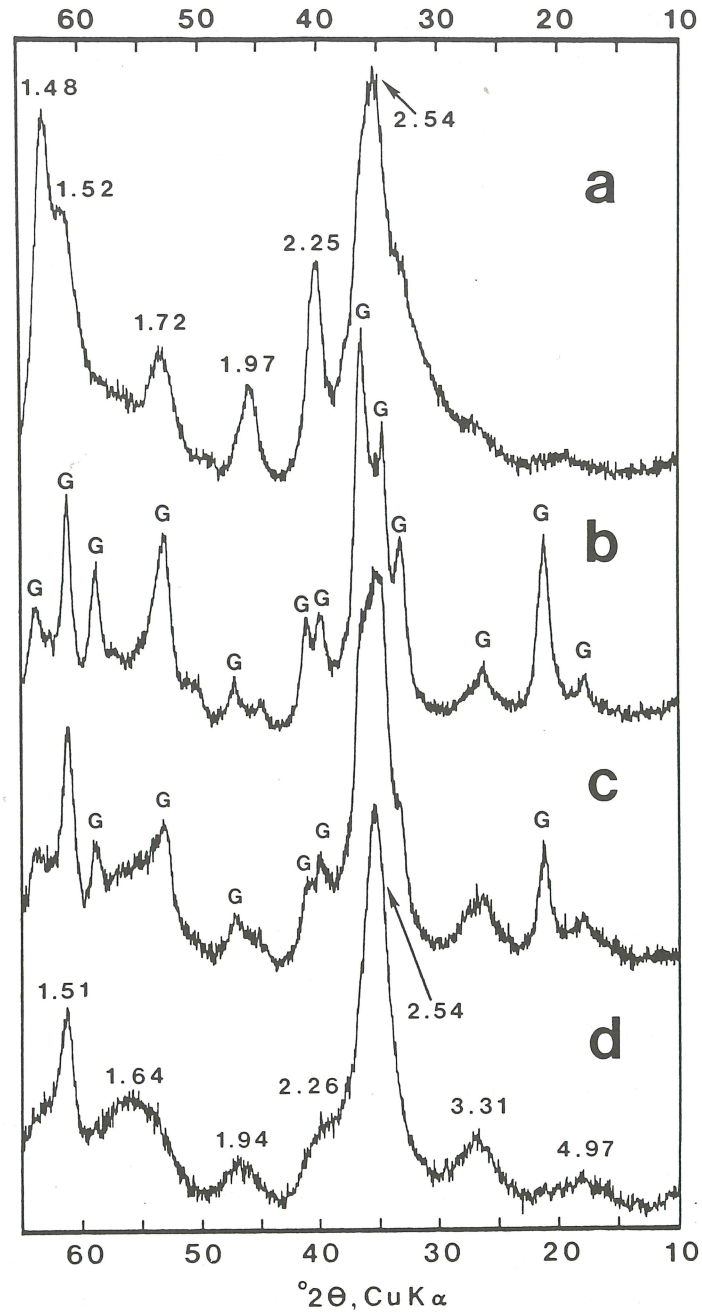

Figure 4.9. X-ray diffraction patterns from synthetic specimens prepared by hydrolysis of ferric nitrate solutions in the presence of (a) 0 mg/L SO_4, (b) 500 mg/L SO_4, (c) 1000 mg/L SO_4, and (d) 2000 mg/L SO_4 (from Brady *et al.*, 1986).

by Bigham *et al.* (1992), jarosite was detected in mine-drainage streams only when [SO4] exceeded 3000 mg/L in the pH range 2.6 to 3.3.

No thermodynamic data are currently available for schwertmannite, but field and laboratory studies suggest that SO_4 concentrations in the range of 1000 to 3000 mg/L are optimal for its formation under the characteristic pH conditions shown in Figure 4.8. Several laboratory studies have also shown SO_4 to enhance the formation of goethite over other iron oxyhydroxides (*e.g.*, lepidocrocite) even though SO_4 is not a structural component of these minerals (Dousma *et al.*, 1979; Brady *et al.*, 1986; Carlson and Schwertmann, 1990). Under field conditions, the precipitation of ferrihydrite seems to be rather insensitive to [SO_4]; however, once ferrihydrite is formed it seems to transform rapidly to goethite in the continued presence of SO_4 (Bigham *et al.*, 1992).

The data presented in Figure 4.9 were taken from an experiment conducted by Brady *et al.* (1986) wherein a series of precipitates were prepared by rapidly hydrolyzing 0.02 *M* $Fe(NO_3)_3$ solutions containing graded amounts of SO_4 (as Na_2SO_4) in the range of 0 to 2000 mg/L. After aging for 30 days in dialysis against distilled H_2O, the precipitates were freeze-dried and analyzed by XRD. When SO_4 was excluded from the hydrolysis solutions, a typical, six-line ferrihydrite was obtained (Figure 4.9a). By contrast, 250-500 mg/L SO_4 facilitated the formation of a poorly crystallized goethite (Figure 4.9b). Further increases in SO_4 to 1000 and 1500 mg/L produced mixtures of goethite and schwertmannite (Figure 4.9c), and only schwertmannite was obtained at 2000 mg/L SO_4 (Figure 4.9d). The XRD patterns shown in Figure 4.9c and d are similar to those presented for the natural materials described in Section 4.4.2. (Figure 4.4 and 4.5a). The natural materials precipitated from drainage waters that had SO_4 concentrations comparable to those utilized in the laboratory synthesis.

4.5.4. Dissolved Carbonate

Most alkaline mine drainage is found in mining districts with abundant limestone or dolomite in the rock column, and the drainage is commonly charged with dissolved carbonate. These conditions might seem to favor the formation of lepidocrocite because procedures for synthesizing this mineral usually involve the oxidation of Fe^{2+} solutions that are buffered in the pH range 5 to 7.5 (Schwertmann and Cornell, 1991). In fact, ferrihydrite and goethite appear to be the normal oxidation products of iron in alkaline mine drainage (Figure 4.8), and this preference is apparently related both to the rate of oxidation and the presence of dissolved carbonate. Whereas rapid oxidation of iron shifts the system toward ferrihydrite, the presence of dissolved carbonate clearly favors goethite.

Both field and laboratory examples are available to demonstrate that goethite

formation is enhanced over lepidocrocite when Fe^{2+} solutions are oxidized in the presence of HCO_3-(Schwertmann and Fitzpatrick, 1977; Fey and Dixon, 1981; Goodman and Lewis, 1981). Recently, Carlson and Schwertmann (1990) observed that the proportion of lepidocrocite to goethite in samples synthesized by oxidizing $FeCl_2$ solutions with air/CO_2 gas mixtures decreased from 100 to 0% as [HCO_3-] increased from 0 to 16 mmol/L (Figure 4.10). These authors also compared infrared spectra from their synthetic specimens with a natural mine-drainage goethite and found that both showed distorted but distinct absorption bands due to CO_3^{2-} (Figure 4.11).

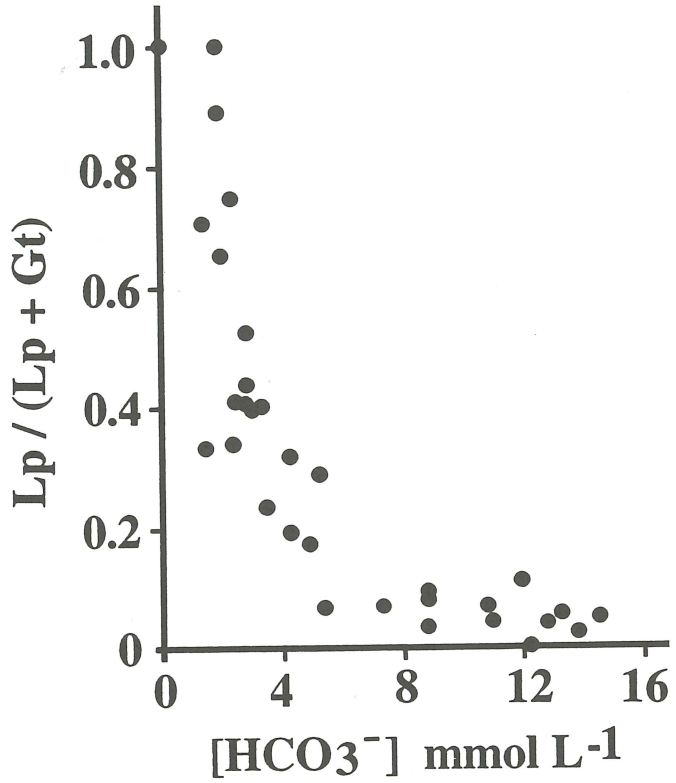

Figure 4.10. Ratio of lepidocrocite to goethite (Lp/Lp + Gt) produced at pH = 6 as a function of [HCO_3-] in solution (modified from Carlson and Schwertmann, 1990).

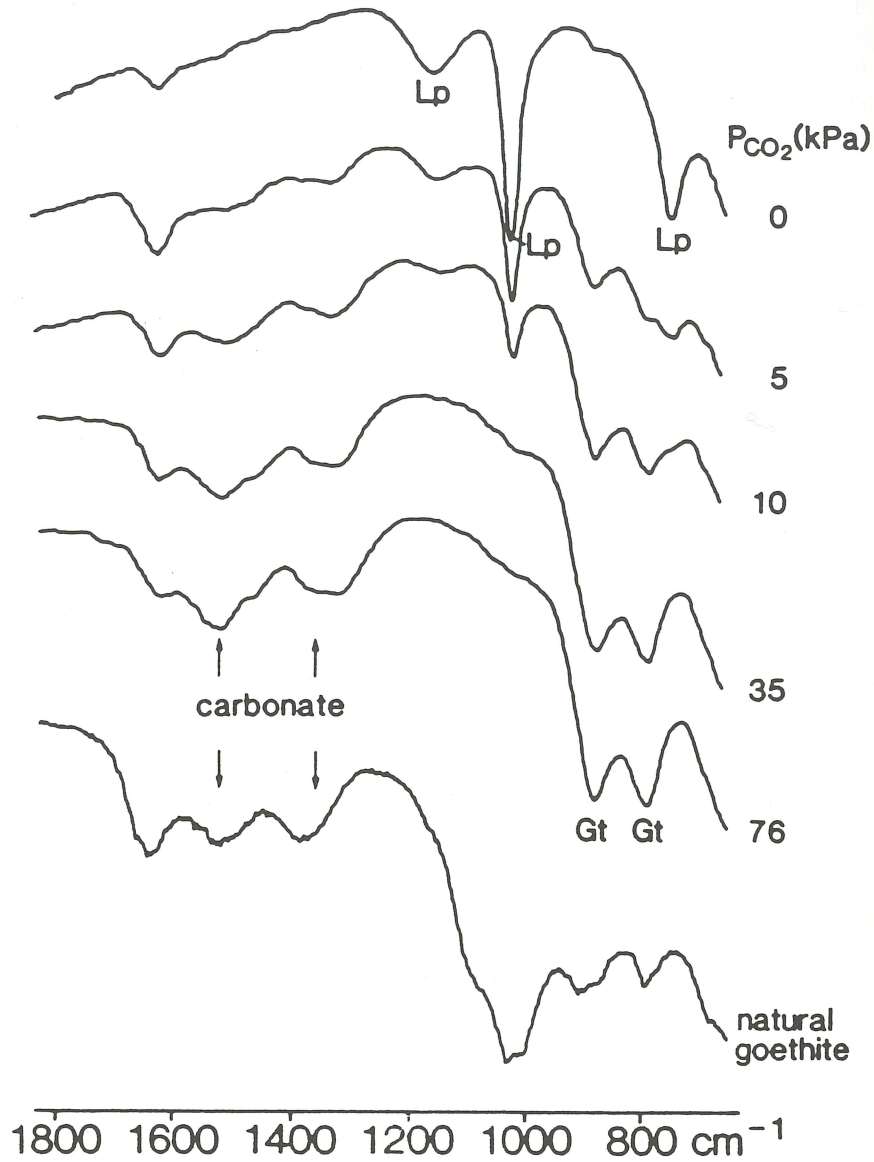

Figure 4.11. Infrared spectra of synthetic specimens prepared at pH 6 and various $P(CO_2)$. Proportion of goethite (Gt) relative to lepidocrocite (Lp) increases from top to bottom. Natural goethite is from mine drainage (from Carlson and Schwertmann, 1990).

4.6. A MODEL FOR MINERAL FORMATION

The previous information regarding mineral speciation in mine-drainage ochres is summarized in Figure 4.12. This "model" is primarily based on field observations and physical data. Consequently, it has a strong kinetic bias with little consideration of solubility controls and other important thermodynamic factors.

According to the proposed model, Fe^{2+} and SO_4^{2-} are released to solution through the bacterially catalyzed decomposition of iron sulfides. A variety of soluble iron sulfates (*e.g.*, melanterite, rozenite) may form as intermediate phases but, ultimately, Fe^{2+} is oxidized and hydrolyzed to form one or more of the minerals associated with mine-drainage ochres. If conditions involving low pH (<3.0), high dissolved SO_4^{2-} (>3000 mg/L), and sustained bacterial activity persist, jarosite or related basic iron sulfates will precipitate in the presence of suitable metal cations. At somewhat higher pH (3.0—4.0) and lower dissolved SO_4^{2-}concentrations (1000 to 3000 mg/L), schwertmannite seems to be the preferred phase. Under these conditions, which are typical of most "acid" mine drainage, bacterial activity is still necessary for rapid oxidation of Fe^{2+}. Slightly acid to alkaline solutions bearing high concentrations of dissolved Fe are conducive to the precipitation of ferrihydrite. Ferrihydrite is clearly a metastable phase whose transformation to other mineral species may be temporarily delayed by contamination of reactive surfaces with organic compounds and adsorbed Si (Childs, 1992). All mineral phases common to ochre deposits are, in fact, transient with respect to goethite, and this is perhaps the most important factor influencing the widespread distribution of goethite in mine-drainage environments. Goethite may also be the primary mineral product formed when low-pH effluents are neutralized by carbonate-charged stream waters.

The proposed model is incomplete with respect to lepidocrocite. Even though lepidocrocite has been documented as a constitutent of ochre deposits associated with sulfide oxidation, the conditions favoring its precipitation are unclear. Synthesis experiments indicate that lepidocrocite formation is favored by the direct, slow oxidation of Fe^{2+}, but is inhibited by low pH, high $[Al^{3+}]$, high $[SO_4^{2-}]$, and high $[HCO_3^-]$. Consequently, it must occupy a rather narrow niche in the total range of mine-drainage environments. Even though the proposed model is not comprehensive, it can perhaps serve as a starting point to understand better the many factors and processes controlling mineral formation in these unique geochemical systems.

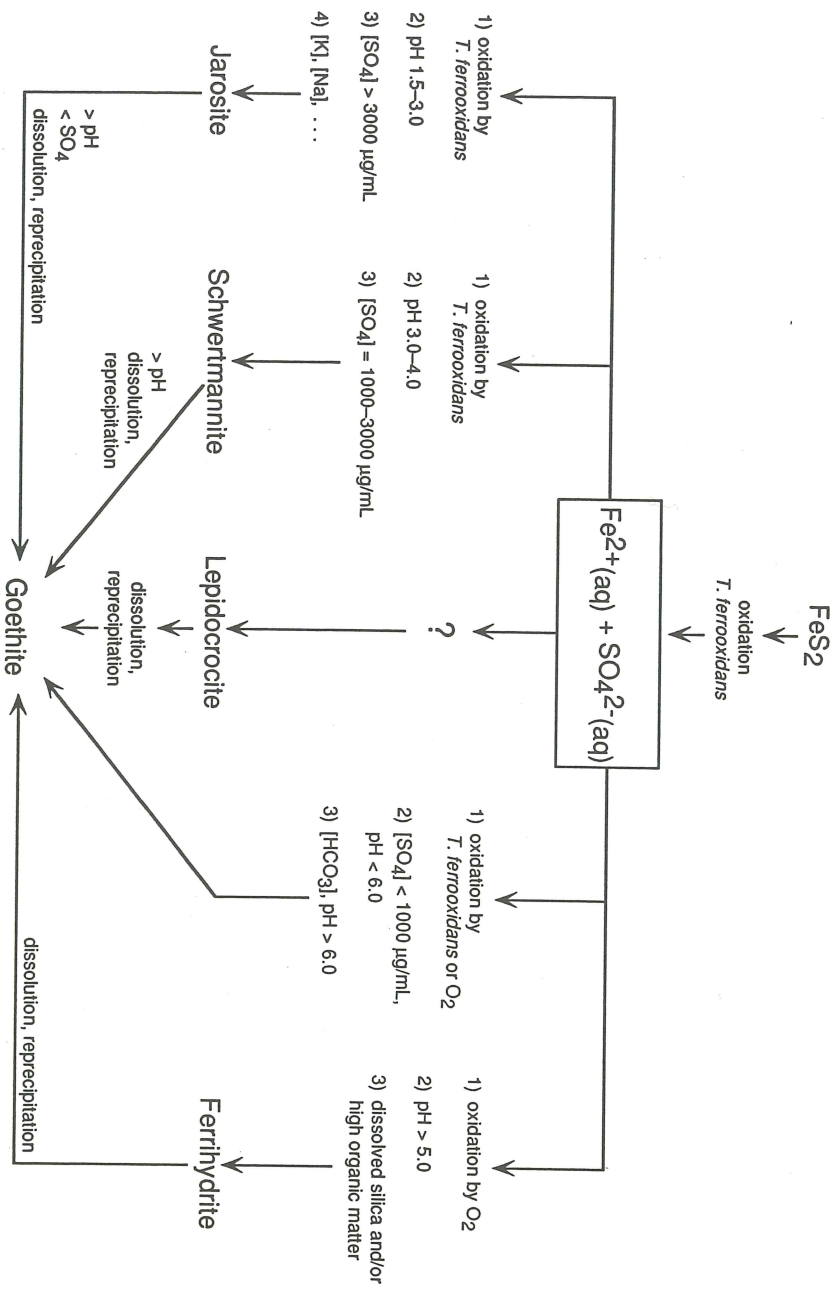

Figure 4.12. Biogeochemical model for the precipitation of various minerals occurring in mine-drainage ochres (modfied from Bigham *et al.*, 1992).

Chapter 5

The Waste-rock Environment

A.I.M. Ritchie
Environmental Science
Australian Nuclear Science and Technology Organization
PMB 1, Menai, NSW 2234 Australlia

5.1. INTRODUCTION

The quantity, chemical composition, and time dependence of polluted drainage from pyritic waste-rock dumps are of considerable concern to environmental regulators and mine operators in many countries around the world. All of these properties reflect the rate of pore-water movement and pore-water chemistry in a dump. The latter, which depends on the pollutant-generation rate within the dump, is driven in turn by the rate of oxidation of pyrite. It is the oxidation of pyrite that is the primary pollutant-generation process. The oxidation rate depends on a number of factors which define the environment within the waste-rock dump, including temperature, pH, oxygen concentration, chemical composition of the pore water, microbial population, and so on. In short, the physico-chemical-microbiological environment within a waste-rock dump determines the pyrite oxidation rate, which in turn determines the physico-chemical-microbiological environment. To predict pollution-generation rates in a waste-rock dump and the consequent chemical composition of pore water, we must know what the environment is and be able to predict what it is or might be when certain conditions are changed.

The environment within a tailings impoundment is determined by similar processes, but there are significant differences between the properties of tailings dams and waste-rock dumps, and these differences have an impact on the environment within each. Chief amongst these is the generally higher height-to-base ratio in a waste-rock dump, and the much coarser run-of-mine material that goes to make up a waste-rock dump. Gas-transport mechanisms, the degree of water saturation, and the intrinsic oxidation rate of the waste material can all be affected by these differences in waste-material properties. This Chapter provides a brief review of the mechanisms and timescales involved in the production of acid drainage from a waste-rock dump, the chemical characteristics of ARD, and the physical characteristics of waste-rock dumps